Zeolite Membranes

International Edition: DOI: 10.1002/anie.201806361
German Edition: DOI: 10.1002/ange.201806361

Uniformly Oriented Zeolite ZSM-5 Membranes with Tunable Wettability on a Porous Ceramic

*Donglong Fu, Joel E. Schmidt, Paul Pletcher, Pelin Karakiliç, Xinwei Ye, Carolien M. Vis, Pieter C. A. Bruijnincx, Matthias Filez, Laurens D. B. Mandemaker, Louis Winnubst, and Bert M. Weckhuysen**

Abstract: *Facile fabrication of well-intergrown, oriented zeolite membranes with tunable chemical properties on commercially proven substrates is crucial to broadening their applications for separation and catalysis. Rationally determined electrostatic adsorption can enable the direct attachment of a b-oriented silicalite-1 monolayer on a commercial porous ceramic substrate. Homoepitaxially oriented, well-intergrown zeolite ZSM-5 membranes with a tunable composition of Si/Al = 25–∞ were obtained by secondary growth of the monolayer. Intercrystallite defects can be eliminated by using Na^+ as the mineralizer to promote lateral crystal growth and suppress surface nucleation in the direction of the straight channels, as evidenced by atomic force microscopy measurements. Water permeation testing shows tunable wettability from hydrophobic to highly hydrophilic, giving the potential for a wide range of applications.*

Zeolite membranes fabricated on porous substrates continue to attract considerable attention from academic and industrial groups because of their potential applications as membranes for separations, catalytic membrane reactors, chemical sensors, components in opto- and microelectronic devices, and uniform model systems for fundamental studies.[1–11] Their performance can be greatly influenced by crystallographic orientation, and the secondary growth method offers a robust approach to control the zeolite membrane orientation by growth of a seeded monolayer.[5,6,12,13] Oriented crystal monolayers are first attached to substrates using manual assembly by surface modification of substrates and/or zeolite crystals to generate chemical bonds,[12,14] hydrogen bonding,[15] ionic linkers,[16] or using water–air interface assembly,[17] and can then be formed into well-intergrown films through secondary growth.[5,13] For the fabrication of oriented membranes with the MFI framework topology—which is globally used in large quantities in petroleum refining and chemical industries—oriented monolayers have been conventionally fabricated on porous substrates; that is, α-Al_2O_3 or homemade SiO_2 substrates.[5,9,13,18] However, coating Al-free MFI (silicalite-1) crystals on porous substrates traditionally requires additional surface functionalization using organics, such as polymers, which serve to adhere the crystals to the substrate.[12,19–21] While the recently developed filter coating and floating particle coating methods can yield closely packed monolayers of silicalite-1, these methods are limited to ultrathin nanosheets.[9,18] Furthermore, reports on the growth of highly *b*-oriented aluminosilicate MFI (ZSM-5) membranes with a tunable Al content supported on porous substrates are scarce, even though this parameter is critical to control the wettability, sorption potential, cation exchange capacity, and concentration of Brønsted acid sites—all of which dictate performance.[7,22–25]

Herein, we use Na^+ as the mineralizer to eliminate intercrystallite defects and form homoepitaxially oriented, well-intergrown zeolite ZSM-5 membranes with a tunable composition of Si/Al = 25–∞ by secondary growth of a silicalite-1 monolayer that is rationally attached on a commercial porous ceramic substrate; that is, mesoporous γ-Al_2O_3-coated α-Al_2O_3, by electrostatic adsorption without surface functionalization or organic coating. It has been conventionally reported that low surface roughness and high concentrations of hydroxy groups (-OH) of the substrates are critical to fabricating highly oriented and robustly attached -OH-rich slicalite-1 monolayers through hydrogen bonding.[13,26,27] The widely used α-Al_2O_3 substrates are cost-effective, but their severe surface roughness (ca. 86.2 nm; Supporting Information, Figure S1) and low -OH concentration (Figure S2) prevent the direct attachment of a uniform layer of oriented crystals (Figure S1). Thus, α-Al_2O_3 substrates with a smooth (roughness of ca. 3.8 nm, Figure 1a) and -OH-rich SiO_2 surface (Figure S2) were tested.[28] However, no continuous monolayer adhered either through manual assembly (Figure 1c) or dip-coating (Figure S3), despite the abundance of -OH in the mixture of silicalite-1 and SiO_2, as demonstrated by the intense IR transmission absorption in the -OH stretching region (Figure S2).[26]

[*] D. Fu, Dr. J. E. Schmidt, Dr. P. Pletcher, X. Ye, C. M. Vis, Prof. Dr. P. C. A. Bruijnincx, Dr. M. Filez, L. D. B. Mandemaker, Prof. Dr. Ir. B. M. Weckhuysen
Debye Institute for Nanomaterials Science, Faculty of Science
Utrecht University
Universiteitsweg 99, 3584 CG Utrecht (The Netherlands)
E-mail: b.m.weckhuysen@uu.nl
Homepage: http://www.inorganic-chemistry-and-catalysis.eu
P. Karakiliç, Prof. Dr. L. Winnubst
Inorganic Membranes, MESA+ Institute for Nanotechnology
University of Twente
7500 AE Enschede (The Netherlands)
Supporting information and the ORCID identification number(s) for the author(s) of this article can be found under: https://doi.org/10.1002/anie.201806361.

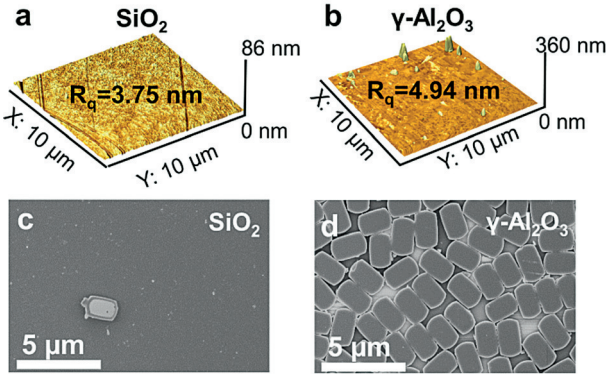

Figure 1. a,b) AFM micrographs of α-Al_2O_3 substrates with SiO_2 (a) and γ-Al_2O_3 (b) surfaces. R_q is the root mean square roughness. c,d) SEM images of silicalite-1 crystals seeded on α-Al_2O_3 substrates with SiO_2 (c) and γ-Al_2O_3 (d) surfaces.

As the best-case scenario of smooth, -OH-rich, SiO_2-coated substrates did not cause attachment of -OH-rich silicalite-1 crystals through hydrogen bonding, another potential force, that is, electrostatic adsorption, was explored. Previous works have shown that an opposite charge between substrates and zeolites, controlled by either pH[29] or an applied electric field,[7,30] can lead to robust attachment. Inspired by these works, we characterized a range of substrate materials dispersed in deionized H_2O using ζ-potential measurements (Table 1). Both SiO_2 and silicalite-1 have negative surface charges, and the mixture of the two shows

Table 1: ζ-Potential measurements of the silicalite-1 and powdered substrates, as well as their mixtures, in aqueous suspensions.

Material	ζ-Potential [mV][a]	Material	ζ-Potential [mV][a]
Silicalite-1	−55.1 ± 1.0	γ-Al_2O_3	+32.9 ± 1.8
α-Al_2O_3	+6.78 ± 1.3	Silicalite-1 + α-Al_2O_3	−30.1 ± 1.8
SiO_2	−2.4 ± 5.9	Silicalite-1 + SiO_2	−34.6 ± 3.5
SiO_2[b]	+18.0 ± 0.7	Silicalite-1 + γ-Al_2O_3	−3.9 ± 0.5

[a] 1 wt% of crystals were dispersed in deionized water to maintain a clear solution. [b] 1 wt% of the SiO_2 powder was dispersed in a pH 4 HCl solution.

a ζ-potential of −34.6 mV that lies between their individual components, revealing a weak interaction of the two materials. In contrast, γ-Al_2O_3 shows a highly positive surface charge, and the mixture with silicalite-1 has a near zero charge (−3.9 mV).[30] This explains why -OH groups alone were insufficient to cause attachment. CO FTIR spectroscopy measurements (Figure S4) demonstrate the different protonation and dissociation abilities of the -OH in these materials, contributing to positively and negatively charged surfaces, respectively.[30,31] We then tested this observation and found that using a commercially available, cost-effective substrate, mesoporous γ-Al_2O_3-coated α-Al_2O_3, with a similar surface roughness (Figures 1b; Figure S5) compared to the SiO_2-coated substrate, could lead to the attachment of a highly *b*-oriented silicalite-1 monolayer (Figure 1d) by manual assembly. The observations are supported by scanning electron microscope images (SEM; Figure 1d) and X-ray diffraction (XRD; Figure S6), where only four peaks of the (010) orientation are observed, which correspond to the (020), (040), (060), and (080) reflections. Moreover, control experiments (Figure S7) further demonstrate that the electrostatic adsorption is responsible for the robust adhesion of silicalite-1 monolayers. This adhesion can even be preserved after sonication (Figure S8)—an approach for testing the strength of zeolite monolayers.[12] Additionally, attachment of a silicalite-1 monolayer on porous substrates by electrostatic adsorption can be extended to other substrates with a negative charge (for example, TiO_2 or a near zero charge substrate such as ZrO_2 (Figure S9)) by manipulating the surface charges with pH.

After finding a method to robustly attach the monolayers to the porous γ-Al_2O_3-coated α-Al_2O_3 substrates, we proceeded with secondary growth to form well-intergrown, *b*-oriented membranes.[13] Previously, it has been reported that, using tetrapropylammonium cation (TPA^+) as the structure-directing agent (SDA), highly *b*-oriented ZSM-5 membranes with Si/Al = 139 could be grown from an Al-free secondary growth medium (SGM) solution where the alumina substrate is an uncontrollable Al source,[13,32] resulting in untunable chemical properties of the membranes for limited applications. Moreover, increasing the Al content to a Si/Al ratio lower than 125 will disrupt the orientation in the TPA-directed membranes.[33] To grow membranes with variable Al contents on the porous substrates, the method we reported to fabricate ZSM-5 films on quartz plates was applied using ethanol added to the SGM, which can be removed at low temperature to avoid crack formation.[33] A well-intergrown (Figure S10b) ZSM-5 membrane was obtained from the SGM with Si/Al = 125, and large defects (Supporting Information, Table S2) that would severely compromise the performance of membranes were found on membranes with Si/Al of 45 (Figure S10a) and ∞ (Figure S10c); the latter might be induced by the non-optimal dissolution of alumina from the substrate. Dissolution suppresses the growth of zeolite crystals because the kinetics of autocatalytic crystallization using ethanol as the organic additive are sensitive to the Al content in the gel, and zeolites would not crystallize at either low or high Al concentrations.[34] The successful SGM solution with Si/Al = 125 may have a composition located in the autocatalytic range after Al dissolution.

To eliminate intercrystallite defects in the membranes with Si/Al = 45 and ∞, NaF (a neutral mineralizing agent that has been used previously in the synthesis of randomly oriented ZSM-5 films without an organic template) was added, and the basic conditions of the SGM solutions were preserved.[22,35] The addition of NaF (total Na^+/Al = 54.4 in the SGM solution, Table S2) led to the formation of a well-intergrown, oriented ZSM-5 membrane in the SGM with Si/Al = 45 (Figure 2b). A well-intergrown ZSM-5 membrane grown from the SGM with Si/Al = ∞ (Figure 2a) could also be prepared using the same absolute amount of NaF. All the membranes are highly *b*-oriented, shown by the XRD results in Figure S11. The relative importance of Na^+ versus F^- was examined by replacing NaF with an identical molar amount of KF, and the results show that KF could not promote growth of

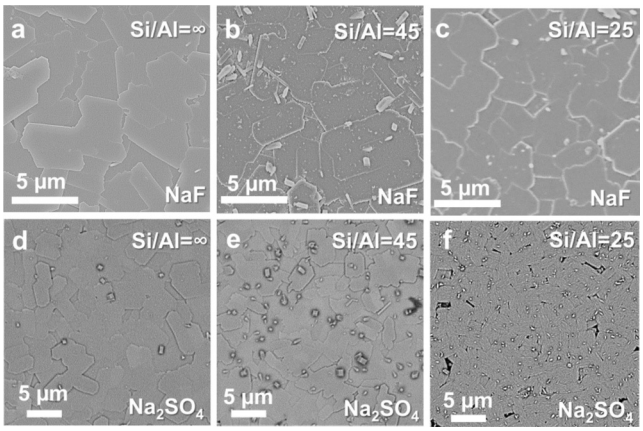

Figure 2. SEM images of zeolite ZSM-5 membranes grown on γ-Al_2O_3-coated α-Al_2O_3 substrates from the SGM solutions with Si/Al ratios of a) ∞, b) 45, and c) 25 using NaF as the additive. d–f) are the SEM images of zeolite ZSM-5 membranes grown from the SGM solutions with Na_2SO_4 as the additive in the same conditions.

zeolite monolayers to form well-intergrown membranes (Figure S12). This demonstrates the important role of Na^+ in the growth of zeolite ZSM-5 membranes.

The safety concerns of NaF could be a showstopper for industrial applications; therefore, Na_2SO_4 was tested as a non-hazardous and cost-effective Na^+ source in the SGM solutions with Si/Al = 45 and ∞. Figure S12 shows that Na_2SO_4 can effectively promote the growth of zeolite monolayers to membranes with only small defects, which can be eliminated in the membranes with Si/Al = ∞ (Figure 2d) and 45 (Figure 2e) using an additional growth step. The same method was also applied for the growth of well-intergrown, highly oriented ZSM-5 membranes with higher Al contents. Compared to the Si/Al = 25 membrane (Figure S13a) grown from an additive-free solution (Na^+/Al = 19.4, from sodium silicate), the addition of NaF, for a total Na^+/Al = 54.4, led to the formation of well-intergrown membranes (Figure 2c). Na_2SO_4 also accelerated the zeolite growth considerably in the SGM with Si/Al = 25, as demonstrated by the formation of well-intergrown films on quartz substrates (Figure S13d) and membranes on γ-Al_2O_3-coated α-Al_2O_3 substrates with only small defects (Figure 2f). Therefore, we confirmed that the anion plays a limited role in the growth of well-intergrown membranes, and while fluoride remains a superior mineralizing agent, the safer substitute used herein leads to similar results; we believe this is an important innovation.

Atomic force microscopy (AFM) was employed to monitor the crystal growth to study the role of Na^+ in the formation of well-intergrown ZSM-5 films with high Al contents.[36–38] Compared to the pristine silicalite-1 crystals, the AFM micrographs in Figure 3 and Figure S14 show that the crystals in the membranes grown in Na^+ additive-free SGM with Na^+ from sodium silicate (Na^+/Al = 19.4) have large terraces on their surface after 2 h of growth, while no apparent terraces were observed on the crystals grown from the SGM with Na^+ additive until the 12 h mark. An analysis of the surface structure was conducted by measuring the step heights along the marked lines (Figure 3; Figure S14). The results show that the crystals grown from Na^+ additive-free SGM always have apparent terraces with a step size of approximately 1.0 nm, which is equal to the height of the building unit of MFI; that is, a pentasil chain.[36] In contrast, the surfaces of the crystals grown from the SGM with NaF and Na_2SO_4 are disordered at 2 h (Figure 3e) and 6 h (Figure S14d), and ordered terraces with pentasil chain steps were obtained only after 12 h (Figure 3f). The disordered-to-ordered surface transformation in Na^+ additive-assisted growth is consistent with a recent study of silicalite-1 growth, revealing the attachment and rearrangement of disordered nanoparticle precursors of silicalite-1 to form ordered structures (that is, terraces).[37] The ordered surface structure growth in Na^+ additive-free SGM is probably the result of the direct attachment of ordered aluminosilicate precursors,[37] and the delayed growth of the ordered terraces (Table S5) as thick as a single unit cell of MFI suggests that the surface nucleation was suppressed by Na^+ additives.[36] Moreover, a faster growth rate along both the *a*- (Figure 3g) and *c*-axes (Figure 3h) was obtained in the SGM with Na^+ additives. As shown in Figure S15, well-intergrown films were

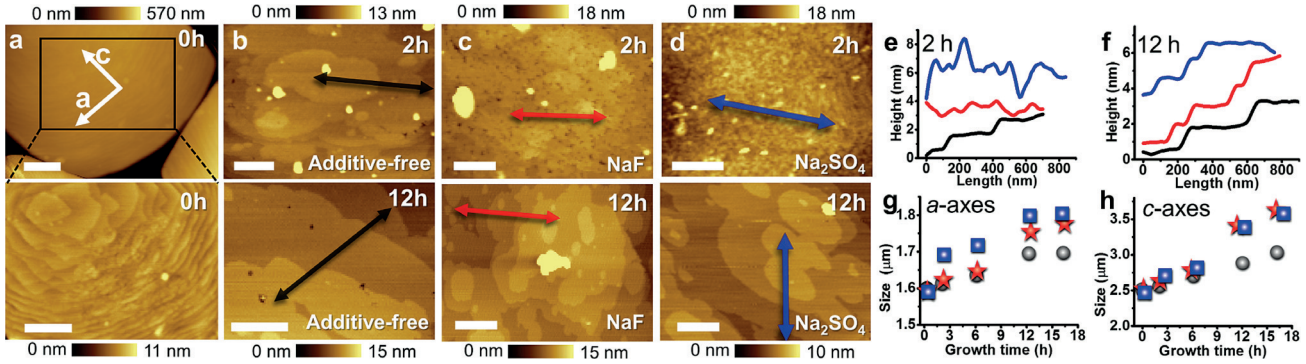

Figure 3. a–d) AFM height micrographs of a) the crystals (top) and their surface (bottom) in silicalite-1 monolayers, as well as zeolite ZSM-5 films grown on quartz plates in the b) additive-free, c) NaF, and d) Na_2SO_4 added SGM solutions with Si/Al = 25. The top and bottom micrographs in (b–d) were obtained after 2 h and 12 h growth, respectively. e,f) Height profiles along the marked lines in (b–d), where the corresponding colors show the growth of terraces with a step size of ca. 1 nm. g,h) Changes in the lateral dimensions along *a*-axes (g) and *c*-axes (h) in the additive-free (gray sphere), NaF (red star), and Na_2SO_4 (blue square) added SGM solutions. Statistics are based on the measurement of at least 50 crystals in each sample. White scale bar: 350 nm.

observed after 20 h of growth in the SGM with Na^+ additives, but large defects can still be observed even after 24 h (Figure S15f) in its Na^+ additive-free counterpart. Similar anisotropic growth rates have also been reported for the growth of silicalite-1 crystals with different morphologies (that is, hexagonal prismatic and leaf-shaped plate-like crystals) that are directed using TPA and the trimer of TPA, respectively, showing that different attachments determine the growth rate of the different faces.[39] It is known from a variety of crystal growth studies that the highest activation energy barrier in zeolite growth is surface nucleation.[40] Therefore, we believe that the Na^+ additives might lead to an increase of the activation barrier to growth in the direction of the straight channels (010), such that their surface nucleation was suppressed. However, the crystal can still grow homoepitaxially in the lateral dimensions, contributing to the elimination of the intercrystallite defects in the membranes.[41] This also suggests that, with uniform structures, zeolite membranes can be used as model systems to study zeolite growth mechanisms.

To use the zeolite membranes for catalysis and separations, the organics (that is, ethanol) must be removed. FTIR spectroscopy measurements (Figure S16) demonstrate that ethanol can be efficiently removed at 423 K under vacuum, thereby avoiding crack formation (Figure S17), which is a known challenge with TPA-directed zeolite membranes. The potential application of the calcined membranes was examined by measuring the time for water permeation. As shown in Figure 4, the oriented ZSM-5 membranes exhibit tunable performance from hydrophobic to highly hydrophilic, illustrated by an order of magnitude decrease of the penetration time from much greater than 180 s to approximately 19 s in the ZSM-5 membrane grown from the Al-free SGM solution and that from Si/Al = 25 SGM, respectively. The tunable wettability, which is believed to correlate with the polarity of the zeolite membranes, coupled with the uniform orientation of the membranes, provides superior control of the separation capabilities for molecules with similar sizes but different quadrupoles; for example, CO_2/H_2 or CO_2/N_2.[32,42]

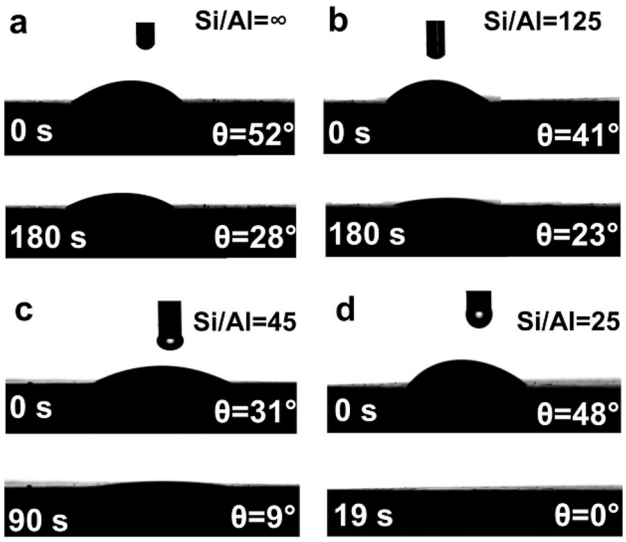

Figure 4. Water/membrane contact angle images from different time frames of the water permeation measurements in ZSM-5 membranes grown on γ-Al_2O_3-coated α-Al_2O_3 substrates from the SGM solutions with Si/Al ratios of a) ∞, b) 125, c) 45, and d) 25 using NaF as an additive. Note that penetration time decreases monotonically with an increase of Al content in the membranes, while initial contact angle does not necessarily correlate with the Al content as the surface properties may not reflect those of the channels.

In summary, we show that zeolite ZSM-5 membranes with a tunable composition of Si/Al = 25–∞ can be fabricated from closely packed monolayers of silicalite-1 and are robustly attached from a rationally proven interaction to a porous ceramic substrate by electrostatic adsorption without organic modification. The membranes exhibit tunable wettability that correlates with the polarity of the zeolite membranes, thereby providing superior control of the separation performance. The addition of Na^+ can lead to the formation of well-intergrown membranes by promoting the lateral crystal growth, while suppressing the surface nucleation to eliminate the intercrystallite defects. The developed method of organic-free monolayer assembly and halogen-free membrane growth on a cost-effective porous ceramic substrate can meet the requirements of scalability, health, and economy, and will serve as a basis to prepare well-defined porous membranes useful for high-flux industrial purposes such as separations and catalysis.

Acknowledgements

This work was supported by a European Research Council (ERC) Advanced Grant (No. 321140), a Gravitation Program of the Netherlands Organization for Scientific Research (NWO), namely Multiscale Catalytic Energy Conversion (MCEC), and Netherlands Technology Foundation (STW-13941). J.E.S. and M.F. have received funding from the European Union's Horizon 2020 research and innovation program under the Marie Sklodowska-Curie grant agreement No. 702149 and No. 748563, respectively. P.C.A.B. received funding from NWO through a VIDI grant. Louis van Bloois, Yanna Liu, and Haili Shi, all from Utrecht University, are thanked for their help with the ζ-potential measurements.

Conflict of interest

The authors declare no conflict of interest.

Keywords: catalysis · inorganic membranes · separation · silicalite-1 · zeolites

How to cite: *Angew. Chem. Int. Ed.* **2018**, *57*, 12458–12462
Angew. Chem. **2018**, *130*, 12638–12642

[1] C. M. Lew, R. Cai, Y. Yan, *Acc. Chem. Res.* **2010**, *43*, 210.
[2] Z. Wang, Y. Yan in *Zeolites in Sustainable Chemistry* (Eds.: F.-S. Xiao, X. Meng), Springer, Berlin, **2016**, pp. 435–472.
[3] P. J. Bereciartua, Á. Cantín, A. Corma, J. L. Jordá, M. Palomino, F. Rey, S. Valencia, E. W. Corcoran Jr., P. Kortunov, P. I. Ravikovitch, A. Burton, C. Yoon, Y. Wang, C. Paur, J. Guzman, A. R. Bishop, G. L. Casty, *Science* **2017**, *358*, 1068.

[4] H. B. Park, J. Kamcev, L. M. Robeson, M. Elimelech, B. D. Freeman, *Science* **2017**, *356*, 1137.
[5] T. C. T. Pham, H. S. Kim, K. B. Yoon, *Science* **2011**, *334*, 1533.
[6] M. Tsapatsis, *Science* **2011**, *334*, 767.
[7] K. Ueno, H. Negishi, M. Miyamoto, S. Uemiya, Y. Oumi, *Microporous Mesoporous Mater.* **2018**, *267*, 1.
[8] X. Shu, X. Wang, Q. Kong, X. Gu, N. Xu, *Ind. Eng. Chem. Res.* **2012**, *51*, 12073.
[9] M. Y. Jeon, D. Kim, P. Kumar, P. S. Lee, N. Rangnekar, P. Bai, M. Shete, B. Elyassi, H. S. Lee, K. Narasimharao, S. N. Basahel, S. Al-Thabaiti, W. Xu, H. J. Cho, E. O. Fetisov, R. Thyagarajan, R. F. DeJaco, W. Fan, K. A. Mkhoyan, J. I. Siepmann, M. Tsapatsis, *Nature* **2017**, *543*, 690.
[10] J. Čejka, A. Corma, S. Zones, *Zeolites and Catalysis: Synthesis Reactions and Applications*, Wiley-VCH, Weinheim, **2010**.
[11] C. Zhou, N. Wang, Y. Qian, X. Liu, J. Caro, A. Huang, *Angew. Chem. Int. Ed.* **2016**, *55*, 12678; *Angew. Chem.* **2016**, *128*, 12869.
[12] B. Zhang, M. Zhou, X. Liu, *Adv. Mater.* **2008**, *20*, 2183.
[13] M. Zhou, D. Korelskiy, P. Ye, M. Grahn, J. Hedlund, *Angew. Chem. Int. Ed.* **2014**, *53*, 3492; *Angew. Chem.* **2014**, *126*, 3560.
[14] S. Y. Choi, Y.-J. Lee, Y. S. Park, K. Ha, K. B. Yoon, *J. Am. Chem. Soc.* **2000**, *122*, 5201.
[15] J. S. Lee, J. H. Kim, Y. J. Lee, N. C. Jeong, K. B. Yoon, *Angew. Chem. Int. Ed.* **2007**, *46*, 3087; *Angew. Chem.* **2007**, *119*, 3147.
[16] G. S. Lee, Y.-J. Lee, K. B. Yoon, *J. Am. Chem. Soc.* **2001**, *123*, 9769.
[17] M. Zhou, J. Hedlund, *J. Mater. Chem.* **2012**, *22*, 3307.
[18] D. Kim, M. Y. Jeon, B. L. Stottrup, M. Tsapatsis, *Angew. Chem. Int. Ed.* **2018**, *57*, 480; *Angew. Chem.* **2018**, *130*, 489.
[19] S. Feng, T. Bein, *Nature* **1994**, *368*, 834.
[20] K. Ueno, Y. Horiguchi, H. Negishi, M. Miyamoto, S. Uemiya, A. Takeno, Y. Sawada, Y. Oumi, *Microporous Mesoporous Mater.* **2018**, *261*, 58.
[21] J. Hedlund, F. Jareman, A.-J. Bons, M. Anthonis, *J. Membr. Sci.* **2003**, *222*, 163.
[22] L. Li, J. Yang, J. Li, J. Wang, J. Lu, D. Yin, Y. Zhang, *AIChE J.* **2016**, *62*, 2813.
[23] M. Ji, G. Liu, C. Chen, L. Wang, X. Zhang, S. Hu, X. Ma, *Appl. Catal. A* **2014**, *482*, 8.
[24] L. Li, N. Liu, B. McPherson, R. Lee, *Ind. Eng. Chem. Res.* **2007**, *46*, 1584.
[25] H. S. Sherry, R. M. Barrer, D. L. Peterson, B. P. Schoenborn, *Science* **1966**, *153*, 555.
[26] J. K. Das, N. Das, S. Bandyopadhyay, *J. Mater. Chem. A* **2013**, *1*, 4966.
[27] Y. Peng, Z. Zhan, L. Shan, X. Li, Z. Wang, Y. Yan, *J. Membr. Sci.* **2013**, *444*, 60.
[28] P. Karakiliç, C. Huiskes, M. W. J. Luiten-Olieman, A. Nijmeijer, L. Winnubst, *J. Membr. Sci.* **2017**, *543*, 195.
[29] L. C. Boudreau, J. A. Kuck, M. Tsapatsis, *J. Membr. Sci.* **1999**, *152*, 41.
[30] B. Oonkhanond, M. E. Mullins, *J. Membr. Sci.* **2001**, *194*, 3.
[31] J. Y. Li, R. K. Xu, *Eur. J. Soil Sci.* **2013**, *64*, 110.
[32] D. Korelskiy, P. Ye, S. Fouladvand, S. Karimi, E. Sjöberg, J. Hedlund, *J. Mater. Chem. A* **2015**, *3*, 12500.
[33] D. Fu, J. E. Schmidt, Z. Ristanović, A. D. Chowdhury, F. Meirer, B. M. Weckhuysen, *Angew. Chem. Int. Ed.* **2017**, *56*, 11217; *Angew. Chem.* **2017**, *129*, 11369.
[34] E. Costa, M. A. Uguina, A. de Lucas, J. Blanes, *J. Catal.* **1987**, *107*, 317.
[35] J. Yang, L. Li, W. Li, J. Wang, Z. Chen, D. Yin, J. Lu, Y. Zhang, H. Guo, *Chem. Commun.* **2014**, *50*, 14654.
[36] M. Shete, M. Kumar, D. Kim. N. Rangnekar, D. Xu, B. Topuz, K. V. Agrawal, E. Karapetrova, B. Stottrup, S. Al-Thabaiti, S. Basahel, K. Narasimharao, J. D. Rimer, M. Tsapatsis, *Angew. Chem. Int. Ed.* **2017**, *56*, 535; *Angew. Chem.* **2017**, *129*, 550.
[37] A. I. Lupulescu, J. D. Rimer, *Science* **2014**, *344*, 729.
[38] M. Kumar, M. K. Choudhary, J. D. Rimer, *Nat. Commun.* **2018**, *9*, 2129.
[39] I. Díaz, E. Kokkoli, O. Terasaki, M. Tsapatsis, *Chem. Mater.* **2004**, *16*, 5226.
[40] L. I. Meza, M. W. Anderson, J. R. Agger, C. S. Cundy, C. B. Chong, R. J. Plaisted, *J. Am. Chem. Soc.* **2007**, *129*, 15192.
[41] J. R. Agger, N. Hanif, C. S. Cundy, A. P. Wade, S. Dennison, P. A. Rawlinson, M. W. Anderson, *J. Am. Chem. Soc.* **2003**, *125*, 830.
[42] M. Pera-Titus, *Chem. Rev.* **2014**, *114*, 1413.

Manuscript received: June 10, 2018
Accepted manuscript online: July 24, 2018
Version of record online: August 20, 2018

